

Spin-aligning ZnMnSe layers and MnSe/ZnSe heterostructures

Heterostructures based on ZnMnSe are used as spin-aligning layers in spintronic devices. To optimize the properties of spin-aligning layers, the structure and Mn distribution in ZnMnSe layers on GaAs (001) with the different Mn concentration in the range from 0 to 100 % were studied. Usually, a ZnSe buffer layer grown on a GaAs(001) substrate is deposited prior to the growth of ZnMnSe. ZnSe occurs in the sphalerite structure with a lattice parameter of 0.566 nm, which is close to that of GaAs (lattice mismatch $\sim 0.27\%$). Bulk MnSe crystals and thick MnSe epilayers are stable in the rock salt structure with a lattice parameter of 0.544 nm (lattice mismatch with respect to ZnSe $f \sim -3.8\%$). The lattice parameter of sphalerite $\text{Zn}_{1-x}\text{Mn}_x\text{Se}$ increases with Mn concentration x and the extrapolated lattice parameter of sphalerite MnSe is 0.590 nm (lattice mismatch between sphalerite MnSe and ZnSe $\sim 4.2\%$). Combining conventional, high-resolution and energy-filtered TEM, the Mn distribution in the ZnMnSe layers and the formation of different phases depending on the Mn concentration are determined.

Fig.1 shows cross-section TEM images of 700 nm thick layers of ZnSe (Fig.1a) and $\text{Zn}_{0.86}\text{Mn}_{0.14}\text{Se}$ layers (Fig. 1b) grown by molecular beam epitaxy (MBE) on GaAs substrates. The ZnSe layer is characterized by a low defect density. There is a dislocation at the ZnSe/GaAs interface but other defects are not observed in the field of view. The incorporation of 14 % of Mn in the ZnSe matrix leads to the generation of V-shaped stacking faults with a density of $\sim 10^9 \text{ cm}^{-2}$ (Fig. 1b).

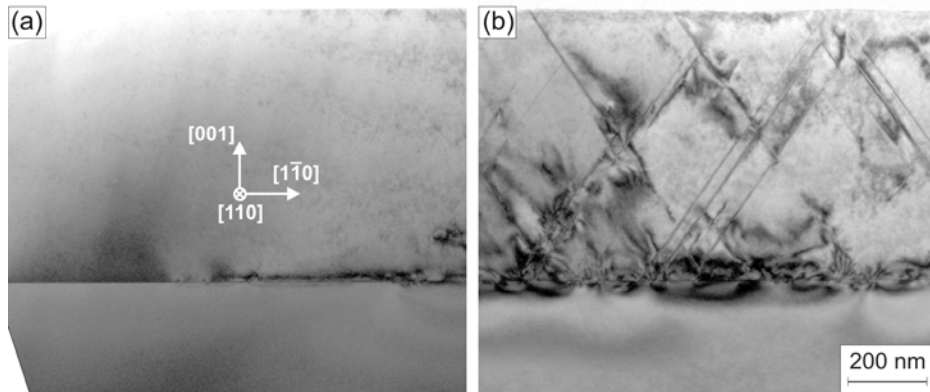


Fig 1: Cross-section bright-field TEM images of 700 nm thick layers of a) ZnSe and b) $\text{Zn}_{0.86}\text{Mn}_{0.14}\text{Se}$ grown on a GaAs (001) substrate taken with $g = (002)$.

It is found that $\text{Zn}_{1-x}\text{Mn}_x\text{Se}$ layers with a thickness of 700 nm and x up to 0.7 occur in the sphalerite structure. Only in a sample with $x = 0.31$ the wurtzite structure was observed. Misfit dislocations with threading segments appear in the $\text{Zn}_{1-x}\text{Mn}_x\text{Se}$ layers with $x > 0.25$, which extend along the [001]-growth direction and have Burgers vectors of the type $\mathbf{b} = \frac{1}{2}\langle 110 \rangle$. Their density increases with the Mn concentration, which can be explained by the increasing strain induced by the lattice parameter misfit f between the substrate and $\text{Zn}_{1-x}\text{Mn}_x\text{Se}$ (f is $\sim 2\%$ at $x = 0.5$). Thick epilayers consisting of pure MnSe contain the fractions of the sphalerite and rock salt phase.

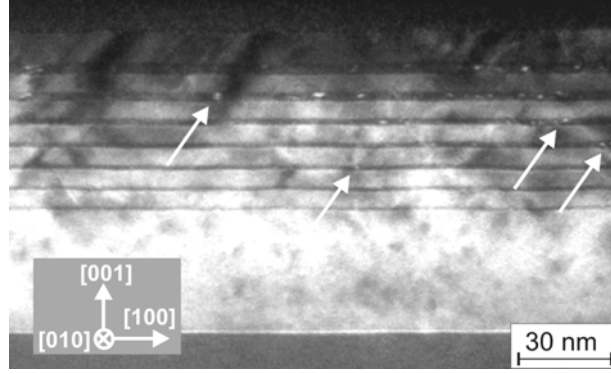


Fig 2: Dark-field TEM image of a [010] cross-section sample taken with $\mathbf{g} = (002)$. The MnSe layers (dark contrast) have a nominal thickness t_{MnSe} of 2 (bottom), 4, 6, 8, 10, 15 and 20 (top) ML.

Another set of samples contained short-period MnSe/ZnSe superlattices with MnSe layers with a thickness between 2 and 20 monolayers (ML). Fig.2 shows an overview (002) dark-field image of the MnSe/ZnSe multiple quantum-well structure. The dark contrast of the (Zn)MnSe layers can be understood by simulations of the amplitude of the chemically sensitive (002) reflection for sphalerite $\text{Zn}_{1-x}\text{Mn}_x\text{Se}$. The (002) amplitude is always lower than for ZnSe in the whole composition range $0 \leq x \leq 1$ independent of the local sample thickness. The Mn concentration of the layers was analyzed carrying out DALI analyses of the local lattice parameter along the [001]-growth direction.

Starting from 6 ML, 5-10 nm small inclusions with bright contrast (arrows in Fig. 2) are observed which represent regions with rock salt structure embedded in sphalerite MnSe. The number and sizes of regions with rock salt MnSe increases with the thickness of the MnSe layers t_{MnSe} . A thickness of 6 ML can be considered as a critical thickness for the epitaxial growth of sphalerite MnSe on ZnSe. The presence of the rock salt structure could be also confirmed by a detailed analysis of diffraction patterns. As for the defects, stacking-fault generation was observed to start at $t_{\text{MnSe}} = 6$ ML. The density of stacking faults increases with t_{MnSe} . Moreover, at the interface between the regions of rock salt MnSe inclusions and sphalerite MnSe, dislocations are observed with Burgers vectors of the type $\mathbf{b} = \frac{1}{2}\langle 110 \rangle$.

References

- [1] M. Hetterich, B. Daniel, C. Klingshirn, P. Pfundstein, D. Litvinov, D. Gerthsen, K. Eichhorn, and D. Spemann, *Lattice parameter and elastic constants of cubic $\text{Zn}_{1-x}\text{Mn}_x\text{Se}$ epilayers grown by molecular-beam epitaxy*, Phys. Stat. Solidi **c1**, 649 (2004)
- [2] D. Litvinov, A. Rosenauer, D. Gerthsen, B. Daniel, and M. Hetterich, *Sphalerite – Rock Salt Phase Transition in ZnMnSe Heterostructures*, Appl. Phys. Lett. **85**, 751 (2004)
- [3] J. Kvietkova, B. Daniel, M. Hetterich, M. Schubert, D. Spemann, D. Litvinov, D. Gerthsen, *Near-band-gap dielectric function of $\text{Zn}_{1-x}\text{Mn}_x\text{Se}$ thin films determined by spectroscopic ellipsometry*, Phys. Rev. **B70**, 045316 (2004)
- [4] Litvinov, D. Gerthsen, B. Daniel, M. Hetterich, C. Klingshirn, *Defects and phase distribution in epitaxial ZnMnSe layers analyzed by transmission electron microscopy*, J. Appl. Phys. **100**, 023523 (2006)